This is an Accepted Manuscript, which has been through the Royal Society of Chemistry peer review process and has been accepted for publication in Green Chemistry. The final authenticated version is published and available online at: https://doi.org/10.1039/C9GC04440J

Early-Stage Evaluation of Emerging CO_2 Utilization Technologies at Low Technology Readiness Levels

Kosan Roh[a], André Bardow[e,c,f,h], Dominik Bongartz[a], Jannik Burre[a], Wonsuk Chung[b], Sarah Deutz[c], Dongho Han[b], Matthias Heßelmann[d], Yannik Kohlhaas[d], Andrea König[a], Jeehwan S. Lee[b], Raoul Meys[c], Simon Völker[c], Matthias Wessling[d,g], Jay H. Lee[b,*], Alexander Mitsos[e,a,f,*]

[a] *Process Systems Engineering (AVT.SVT), RWTH Aachen University, Forckenbeckstraße 51, 52074 Aachen, Germany*

[b] *Department of Chemical and Biomolecular Engineering, Korea Advanced Institute of Science and Technology (KAIST), 291 Daehak-ro, Yuseong-gu, Daejeon 34141, Republic of Korea*

[c] *Institute of Technical Thermodynamics (LTT), RWTH Aachen University, Schinkelstraße 8, 52062 Aachen, Germany*

[d] *Chemical Process Engineering (AVT.CVT), RWTH Aachen University, 52074 Aachen, Germany*

[e] *JARA-ENERGY, 52056 Aachen, Germany*

[f] *Institute of Energy and Climate Research - Energy Systems Engineering (IEK-10), Forschungszentrum Jülich GmbH, 52425 Jülich, Germany*

[g] *DWI-Leibniz Institute for Interactive Materials, Forckenbeckstraße 50, 52074 Aachen, Germany*

[h] *Department of Mechanical and Process Engineering, ETH Zurich, Tannenstrasse 3, 8092 Zürich, Switzerland*

*Corresponding authors: *jayhlee@kaist.ac.kr; amitsos@alum.mit.edu*

Abstract

Most CO_2 utilization technologies are at low technology readiness levels (TRLs). Given the large number of potential technologies, screening to identify the most promising ones should be conducted before allocating large R&D investment. As these technologies exhibit different levels of technical maturity, a systematic, TRL-dependent evaluation procedure is needed which can also account for the quality and availability of data. We propose such a systematic and comprehensive evaluation procedure. The procedure consists of three steps: primary data preparation, secondary data calculation, and performance indicator calculation. The procedure depends on the type of CO_2 utilization technology (thermochemical, electrochemical, or biological conversion) as well as the TRL (2–4). We suggest databases, methods, and computer-aided tools that support the procedure. Through four case studies, we demonstrate the proposed procedure on emerging CO_2 utilization technologies, which are of different types and at various TRLs: electrochemical CO_2 reduction for ten chemicals production (TRL 2); co-electrolysis of CO_2 and water for ethylene production (TRL 2–4); direct oxidation of CO_2-based methanol for oxymethylene dimethyl ether (OME_1) production (TRL 4); and microalgal biomass co-firing for power generation (TRL 4).

Keywords

CO_2 utilization; early-stage evaluation; technology readiness level; ethylene; oxymethylene dimethyl ether; microalgal biomass co-firing

1. Introduction

CO_2 utilization (CU) has attracted much attention by both industry and academia due to its potential to mitigate greenhouse gas (GHG) emissions while generating economic benefits. CO_2 captured from a process stream or air is used either physically, e.g., for enhanced oil recovery, or (bio)chemically, i.e., converted into another species [1]. Limitations of CU technologies often include the small market demand compared to the global GHG emissions [2] and re-emission of carbon dioxide to the atmosphere after the utilization of the product, e.g., for synthetic fuels [3]. Nevertheless, CU may lead to a less carbon-intensive chemical industry [4] and also promote the transition to a sustainable transportation sector [5].

CO_2 can be used as feedstock for a plethora of products [6] through multiple reactions and processing pathways [7]. Some CU processes already exist at a scale larger than pilot, in particular methanol (MeOH) production via CO_2 hydrogenation [8], synthetic methane production via CO_2 methanation [9], and synthetic liquid fuel production via reverse water gas shift technology [10]. Most of the other CU technologies are, however, at low technology readiness levels (TRLs) [1]. The corresponding publications focus on proof of concept for key utilization mechanisms and on CO_2 conversion catalysts [11]. Thus, it is essential to identify promising CU products and corresponding reactions and processing pathways out of the plenty number of the emerging candidates via so-called *early-stage* evaluation.

Successful early-stage evaluation can identify promising technologies to guide R&D investment. Thereby overall cost can be reduced drastically since large-scale experiments and demonstration at higher TRLs are by far the highest cost components in process development [12]. However, such an evaluation is challenging due to limited data available at the early stage. Furthermore, those data may entail either endogenous (e.g., measurement data in experiments) or exogenous (e.g., the future market demand and price of target products) uncertainty, that can result in suboptimal process design, operation and thus performance.

Several previous works have addressed the problem of assisting and even standardizing the evaluation of CU technologies. Otto et al. [6] used the reaction stoichiometry to screen candidates by scoring-based methods. Black [13] proposed performance indicators for the evaluation of CO_2 capture, utilization, and storage technologies in terms of performance, cost, GHG emissions, market, and safety. Schakel et al. [14] proposed a performance indicator representing the energy efficiency of CU technologies concerning fossil feedstock replacement. Roh et al. [15] highlighted three key metrics for the evaluation of CU technologies, including net CO_2 emission, CO_2 avoidance cost, and CO_2 reduction rate. Zimmermann et al. [12] developed a comprehensive guideline for techno-economic analysis (TEA) and life cycle assessment (LCA) tailored to CO_2 capture and utilization. Albrecht et al. [16] developed a standardized TEA methodology for alternative fuels including CO_2-based liquid fuels. Bergerson et al. [17] provided guidance and evaluation techniques for conducting LCA of emerging technologies considering technology and market maturities. Thomassen et al. [18] introduced a framework to assess the techno-economic and environmental potential of mature as well as emerging technologies. However, none of the previous studies have yet thoroughly considered the maturity level of CU technologies in their evaluation. A remaining challenge is how to conduct the early-stage evaluation of emerging CU technologies in the presence of limited and uncertain data.

We propose a procedure for early-stage performance evaluation of emerging CU technologies at early development stages. More specifically, we employ the TRL scale used by the EU[19] and focus on TRL 2 to 4. We use suitable performance indicators and tailor them to three representative types of CU technologies, namely, thermochemical, electrochemical, and biological CO_2 conversion. In Section 2, we describe what primary data are required as input, how to calculate secondary data based on the primary data collected, and how to derive the selected performance indicators. In addition, we suggest various databases, methods, and computer-aided tools that can facilitate the implementation of the procedure proposed. In the following sections, we present four case studies to assess specific emerging CU technologies as well as to demonstrate the use of the proposed procedure. In Section 3, we analyze the potential of ten different value-added products from electrochemical CO_2 reduction at TRL 2 to exclude unpromising ones. In Section 4, we

analyze electrochemical production of ethylene via co-electrolysis of CO_2 and water in order to show how the evaluation procedure and results evolve with respect to TRLs. In Section 5 and 6, we analyze oxymethylene dimethyl ether (OME_1) production via direct oxidation of CO_2-based methanol and microalgal biomass co-firing for power generation, respectively. The two technologies are considered to be at TRL 4 and represent thermochemical and biological CO_2 conversion technologies.

2. TRL-Specific Procedure for Early-Stage Evaluation

For the successful early-stage evaluation of emerging CU technologies at low TRLs, appropriate questions should be asked first. Herein, TRL 2, 3, and 4 are of interest and they are elaborated in Section 1.1 of the Electronic Supplementary Material (ESI). The questions differ according to the TRL. According to Thomassen et al. [18], at TRL 2, we should ask if a given technology is sustainable assuming ideal, i.e., best-case performance, and what the bottlenecks are. Herein, we define "sustainable" for CU technology as being economically viable and also capable of mitigating GHG emissions simultaneously. If the answer to the first question is YES, the technology deserves further research. At TRL 3 and 4, given the proven (TRL 3) or validated (TRL 4) concept, we can ask if the technology is still sustainable and what the bottlenecks for further improvement are. Directions of the further research depend on the answers.

Answering all these questions should be supported by appropriate performance indicators. We use *primary* and *secondary* data to calculate the performance indicators for CU technologies at the low TRLs. Primary data include TRL-dependent data, such as feasible operating conditions and single-pass conversion observed in experiments, and TRL-independent data, such as *known* thermodynamic properties of pure compounds, price data, and carbon emission factors. Secondary data are those calculated by using primary data, such as equipment sizes or energy demand at the *process level*. Performance indicators, calculated by using secondary data and TRL-independent primary data, are categorized into five types: material, energy, economics, GHG reduction, and combined economics and GHG reduction. Figure 1 illustrates how the

primary data, secondary data, and performance indicators are related with one another and how they change when the TRL increases.

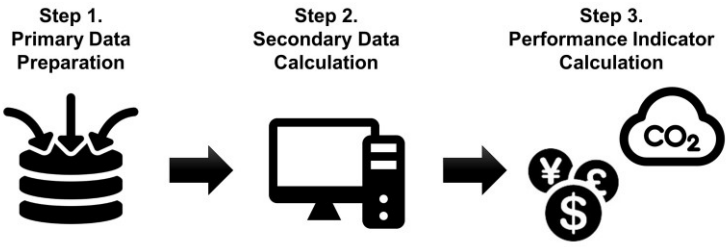

Task description	Collect/generate input data required for Step 2 and 3	Using the primary data, analyze the technology to generate input data required for Step 3	Calculate performance indicators for the technology assessment
As TRL increases	More data available	More complicated the analysis	More certain the indicators
Type of outcome	TRL-dependent data TRL-independent data	Mass balance Energy demand Equipment size	Material & energy indicator Economic indicator GHG reduction indicator Combined GHG reduction-economic indicator

Figure 1. Overview of the procedure for the early-stage evaluation of CO_2 utilization technologies.

2.1 What Primary Data Are Available at Low TRLs?

2.1.1 TRL-Dependent Primary Data

In Table 1 we show available primary data for each TRL and CO_2 conversion type, based on our experience with the analysis of such systems and the TRL specifications in Buchner et al. [20]. Typically, more primary data are available at higher TRLs. Some data are available in existing databases (see Table

SI 3), while others must be obtained by laboratory experiments. More details are described in Section 2.1 of the ESI.

Table 1. Examples of TRL-dependent primary data of CO_2 utilization technologies available at low TRLs. The primary data obtained at lower TRLs are available at higher TRLs.

TRL	Data type	Available primary data
2	Physical properties of participating components	[Common data] - Standard enthalpies of formation - Standard entropies - Specific chemical exergy
3	Lab-scale experimental data measured at a wide range of conditions with various catalysts and small equipment	[Common data] - Feasible temperature and pressure range - Feed specification - Reaction conversion - Selectivity - Residence time - Type and size of actual experimental apparatus - Recovery ratio at separators - Options for unit operations identified [Electrochemical CO_2 conversion only] - Voltage - Current density - Faradaic efficiency - pH [Biological CO_2 conversion only] - Productivity - Yield - pH - Specific energy consumption of unit operations
4	Lab-scale experimental data measured at optimized conditions (i.e., narrower ranges) with enhanced catalysis, bigger equipment, and improved operation	- Updated of the data available at TRL 3 - Unit operations detailed and respective equipment selected

2.1.2 TRL-Independent Primary Data

The TRL-independent primary data can be classified into four categories: reaction and component, market and business, carbon emission factors, and energy. The data may have significant temporal and/or spatial variation, e.g., crude oil price or carbon footprint of natural gas acquisition. Price indices (e.g., ICIS Petrochemical Index [21]) and chemical plant cost indices (e.g., Chemical Engineering Plant Cost Index [22])

can be used to ensure the reliable primary data in the market and business category. The list of TRL-independent primary data related to CU technologies are given in Table SI 1.

2.2 How is Secondary Data Generated?

Table 2 represents our suggested strategy for calculating secondary data. The strategy highly depends on the conversion type and processing tasks (e.g., reaction and separation). At higher TRLs, we consider more elaborate flow diagrams, so a more complicated analysis is required. Essentially, available experimental data should be used. Otherwise, one can rely on simulation or idealized assumptions. Table 2 is elaborated in Section 2.3 of the ESI.

Table 2. Recommended strategies for calculating the secondary data of CO_2 utilization technologies at low TRLs.

TRL		Mass balance	Energy demand	Equipment size	Flow diagram
2	Reaction	100% reaction conversion without any undesirable side reaction	[T] Enthalpy of reaction at standard conditions [E,B] Gibbs free energy change	Exclude	N/A
	Separation	Perfect separation	Exclude		
3[a]	Reaction	Experimental data; [T] reaction conversion and selectivity [E] reaction conversion and Faradaic efficiency [B] yield and productivity	[T] Actual enthalpy of reaction at suggested conditions [E] Electric power based on applied voltage and measured current density [B] Energy demand based on experimental data	Estimation based on the size of actual experimental apparatus if available. Otherwise, approximate sizing based on process simulation. Only major equipment such as reactors and separation units is considered.	Block flow diagram
	Separation	Experimental data or perfect separation	Experimental data or minimum separation work		
	Etc.	Recycle unreacted components	Energy demand for pressurizing vapor feed streams		
4[a]	Reaction	Same as TRL 3	Same as TRL 3	Estimation based on the size of actual experimental apparatus if available. Otherwise, approximate sizing based on process simulation. Minor equipment such as heat exchanges, pumps, etc. is considered in addition to major equipment.	Process flow diagram
	Separation	Experimental data, process simulation, or perfect separation	Experimental data, process simulation, or short-cut methods		
	Etc.	Recycle unreacted components Consider off-gas treatment	Energy demand for pressurizing, heating, and cooling process streams Heat integration		

[T] Thermochemical conversion, [E] Electrochemical conversion, [B] Biological conversion.
[a] Douglas' hierarchical procedure for process synthesis [23] is useful at TRL 3 and 4.

2.3 Performance Indicator Calculation

Based on the primary and secondary data, we assess the feasibility of CU technologies using the performance indicators listed in Table 3. As highlighted in Figure 1, we need more input data to calculate the indicators at higher TRLs, and consequently, the estimates are more reliable. For instance, only direct operating costs (DOC) are calculated for TRL 2 technologies, whereas depreciation costs (arising from capital investment) are added to the DOC for TRL 3 or 4 technologies. Note that the indicators available at TRL 2 imply the theoretical limit, e.g., minimum DOC or maximum possible GHG reduction.

Material and energy indicators require the least amount of input data. These indicators provide a simple way to quickly evaluate CU technologies. They are relevant since costs and carbon footprints of feedstock and energy often dominate those of other elements.

GHG reduction indicators and economic indicators can be calculated by conducting LCA and TEA, respectively. Both are data-intensive and are inherently more uncertain than the material and energy indicators because the former rely on the latter and also introduce uncertainty arising from the additional calculations (e.g., capital cost calculation) and parameters (e.g., lifecycle inventory data).

GHG avoidance cost is a comprehensive and widely usable indicator for the technology evaluation when the target CU technology incurs net costs but can abate GHG emissions. In particular, this indicator can be used for the comparison between different types of CU technologies or even the comparison of CU with CO_2 capture and storage (CCS). In spite of its usefulness, this indicator is the most data-intensive measure as both the GHG reduction and economic indicators are needed. Therefore, this indicator can be highly uncertain. Depending on how the new technology is implemented (new installation vs. retrofitting), the calculation formula for GHG avoidance cost should be distinguished, as represented in Table 3.

All the performance indicators are elaborated in Section 2.4 of the ESI.

Table 3. Performance indicators for the early-stage evaluation of CO_2 utilization technologies at low TRLs.

Category	**TRL**	
	2	**3 & 4**
Material	*Carbon utilization efficiency* = Amount of carbon in the marketable products ÷ Amount of carbon input	
Energy	*Primary energy (or exergy) efficiency*[a] = Net primary energy (or exergy) output ÷ Net primary energy (or exergy) input	
	Specific primary energy consumption = Net primary energy input ÷ FU[b]	
GHG reduction	*Carbon footprint of the CU product* = (GHG emissions throughout the life cycle of the CU process from cradle-to-gate[c,d] including CO_2 capture – CO_2 feedstock) ÷ FU[b]	
	Specific GHG reduction = (GHG emissions of an alternative or benchmark process to be replaced by the CU process – Carbon footprint of the CU product) ÷ FU[b]	
	GHG reduction potential = Specific GHG reduction × Product market demand	
Economics	*Direct operating cost (DOC)* = Raw material cost + Energy and utility cost	*Cost of goods manufactured (COGM)* = DOC + Indirect operating cost (IOC)[e] + Depreciation cost
	Gross operating margin (GOM)[f] = Revenue – DOC	*Specific profit*[f] = Revenue – COGM
Combined GHG reduction and economics	New installation[g]	
	GHG avoidance cost = – GOM ÷ Specific GHG reduction	*GHG avoidance cost* = – Specific profit ÷ Specific GHG reduction
	Retrofitting[h]	
	GHG avoidance cost = (GOM before retrofitting – GOM after retrofitting) ÷ (Carbon footprint before retrofitting – Carbon footprint after retrofitting)	*GHG avoidance cost* = (Specific profit before retrofitting – Specific profit after retrofitting) ÷ (Carbon footprint before retrofitting – Carbon footprint after retrofitting)

[a] If the final product is not considered as a fuel but others such as a chemical feedstock, use specific primary energy consumption as the energy indicator.
[b] Functional unit, which is a measure of the function of the target process (or system).
[c] Cradle-to-gate: a part of the product life cycle ranging from resource extraction to the manufacture plant (before the product is transported to the customer).
[d] Carbon footprints in construction and reconstruction of CU processes are excluded at TRL 2.
[e] Include if reliable values are available.
[f] Only valid when the market price of the main product is set.
[g] Only valid when GOM or specific profit is negative but specific GHG reduction is positive.
[h] Only valid when GOM or specific profit is reduced but GHG emissions are reduced after retrofitting.

2.4 Databases, Methods, and Computer-aided Tools for Assisting the Evaluation Procedure

The proposed evaluation can be conducted with the aid of various databases, methods, and computer-aided tools, as listed in Table 4. For instance, one can access databases of property data for pure components and mixtures to acquire some primary data. Short-cut methods, such as the Rectification Body Method (RBM) [24] for estimating minimum separation energy, facilitate calculation of the secondary data. We can implement block flow diagram (BFD) and process flow diagram (PFD) in numerous process simulators to calculate mass balances and energy demands. Calculation of the performance indicators tailored for CU technologies can be supported by the use of software, for instance, ArKa-TAC^3 [15].

Table 4. Databases, methods, and computer-aided tools applicable to the CU technology analysis and evaluation. The literature and website relevant to each item are given in Table SI 3 of the ESI.

Task	**Type**	**Name**
Stoichiometry analysis	Database	Reaxys®
		SciFinder®
		DIPPR®801
		DDBST
		DETHERM
		NIST Chemistry WebBook
Process flowsheeting, simulation, and optimization	Tool	Aspen Plus®
		Aspen HYSYS®
		PRO/II®
		CHEMCAD
		SuperPro Designer®
		ProCAFD
		FSOpt
Thermodynamic and physical property prediction	Tool	ProPred
		COSMOtherm
		Aspen Plus®
Minimum separation energy prediction	Tool	EE-Toolbox
	Method	RBM
LCA	Tool	ecoinvent
		SimaPro
		GaBi
		LCSoft
		GEMIS
TEA	Tool	APEA
		ECON
		ESTEA
Combined LCA-TEA	Tool	ArKa-TAC^3

		TIPE-CCUS
Monte Carlo simulation	Tool	@RISK
Optimization	Tool	GAMS
		FICO® Xpress
		Pyomo
Network synthesis	Method	RNFA
		PNFA

An effective way of evaluating multiple CU technologies is given by early-stage optimization-based screening methods. Typically, many alternative reaction pathways and process schemes for a given CU product are conceivable. These options can be aggregated to a so-called superstructure [25], which can be optimized with respect to one or multiple objectives, chosen from the performance indicators listed in Table 3. Depending on the TRL, such methods for high-throughput pathway evaluation can mainly be based on primary data or can require *a priori* calculation of secondary data. At TRL 2, examples for screening approaches relying on primary data, e.g., yield and stoichiometry, include a shortcut method for the synthesis and screening of integrated biorefineries by Bao et al.[26] as well as Reaction Network Flux Analysis (RNFA) proposed by Voll et al. [27]. At TRL 3 to 4, incorporating downstream processing steps, Process Network Flux Analysis (PNFA) is proposed by Ulonska et al. [28] as an extension of RNFA, which also requires a priori secondary data calculation, i.e., energy demands for separations. When the considered conversion steps are mature enough such that operating temperatures are known, heat integration can also be included in the optimization [29]. So far, several studies [2,4,30,31] have applied the optimization-based methods to a number of CU pathways comprising of mostly high TRL technologies for producing fuel and/or bulk chemicals in order to identify economically and/or environmentally promising pathway(s) and estimate the GHG reduction potential. Nevertheless, many other emerging products (e.g., polymers and carbonates), reactions, and processing pathways still remain to be analyzed.

3. Case Study 1: Evaluation of Electrochemical CO_2 Reduction Technologies for the Production of Ten Chemical Compounds (TRL 2)

We evaluate the production of ten chemical compounds via electrochemical CO_2 reduction. We herein focus on how to analyze multiple options and exclude unpromising ones using as few primary data as possible.

3.1 Technology Description

Electrochemical CO_2 reduction operating on renewable electricity, illustrated in Figure 2, is a currently widely considered option in a variety of contexts, e.g., energy storage [32] and production of chemical compounds [33]. Electrolysis efficiency is characterized by cell overpotential and current density while selectivity is termed Faradaic efficiency.

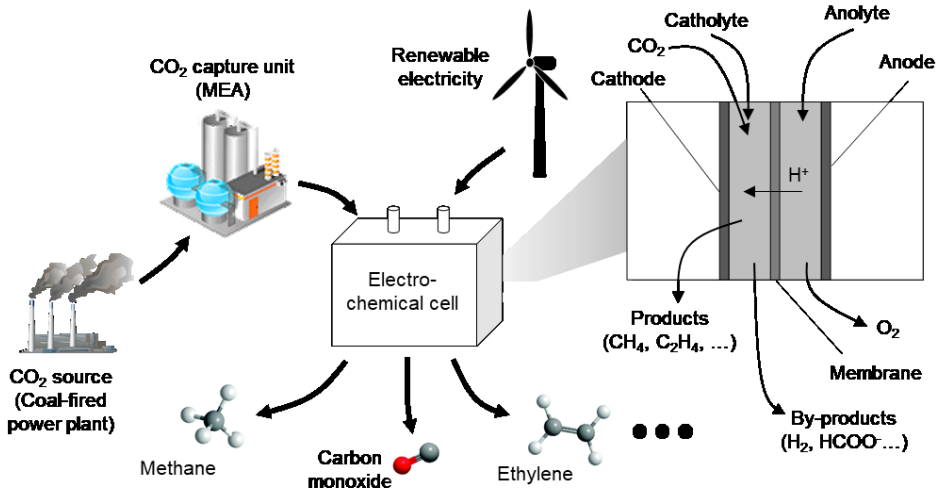

Figure 2. Illustration of the electrochemical CO_2 reduction system and the electrolyzer.

We evaluate ten chemical compounds assumed to be directly produced via electrochemical CO_2 reduction in a cell: carbon monoxide, formic acid, formaldehyde, methane, methanol, ethylene, ethane,

ethanol, oxalic acid, and propanol. Such technologies are considered as being at TRL 2. Thus we evaluate the theoretical limit of their performances by following the proposed evaluation procedure when all the CU products as well as the byproduct oxygen (O_2) are produced and sold in South Korea. South Korea is a suitable country due to several reasons: It was the 8th biggest GHG emitting country in 2018 (659 Megatons of CO_2 equivalent [34]), it imports most of the target chemical compounds (e.g., formic acid, methane, and methanol) as well as fossil fuels, and its government policy aims to increase the ratio of renewable energy generation [35].

The CO_2 feedstock is captured at a coal-fired power plant by using monoethanolamine (MEA) solvent, which is a conventional post-combustion CO_2 capture technology. On-shore wind farms supply renewable electricity to the electrolyzer cells.

3.2 Primary Data Preparation

Most primary data (except for basic thermodynamic properties of components) required at this TRL is TRL-independent, including the stoichiometry, number of electrons, the price and carbon footprint of raw materials, products, and utilities. All data are listed in Tables SI 4–6 of the ESI.

3.3 Secondary Data Calculation

We assume complete conversion and selectivity expressed by Faradaic efficiency, so the effluent stream contains only the target component (i.e., 100% purity). Also, we assume 100% second-law efficiency, implying that the applied potential is equal to open-circuit potential. Note that simplistically the cell is considered as a thermodynamic black box.

3.4 Evaluation Results

The functional unit is 1 ton of the main product and X ton of oxygen byproduct. The value of X depends on what main product is produced. Specific GHG reduction and gross operating margin are calculated for

the evaluation. Material and energy indicators cannot help to exclude unpromising options because they represent ideal performances. We define a cradle-to-gate system boundary for LCA and calculate carbon footprints of both the ten CU products and their alternatives. The size of oxygen market is assumed to be unlimited. The prices of the raw materials, products, and utilities except the renewable electricity are based on the current market in South Korea. For the renewable electricity price, we take the levelized cost of electricity (LCOE) of on-shore wind estimated in South Korea for the year 2030.

The evaluation results (Figure 3) can be used to exclude unpromising products by fast screening. Carbon monoxide, formic acid, formaldehyde, and n-propanol are attractive products as they give both positive specific GHG reduction and positive gross operating margin. Producing ethylene, methanol, methane, ethanol, or ethane mitigates GHG emissions but results in net incurred costs so that we can compare these CU options with CCS. As shown in Figure 3, the GHG avoidance costs of the methane and ethane productions exceed that of CCS, which typically ranges from 46–99 USD/ton-CO_2 with geologic storage [36]. In terms of GHG reduction potential, the CO_2-based ethylene, ethanol, and methane are promising because of their large market size (>10^8 t-Prod/yr). Despite the highest specific GHG reduction and gross operating margin, the CO_2-based propanol is less promising due to its small market demand (~10^5 t-Prod/yr). Oxalic acid yields a negative specific GHG reduction since oxalic acid is commercially produced from biomass feedstock, which originates from atmospheric CO_2. Hence, ethane and oxalic acid are at present not promising CU products in South Korea. We note that a more robust way to identify unpromising technologies at TRL 2 would be to consider the possible ranges of the market and business data and carbon emission factors.

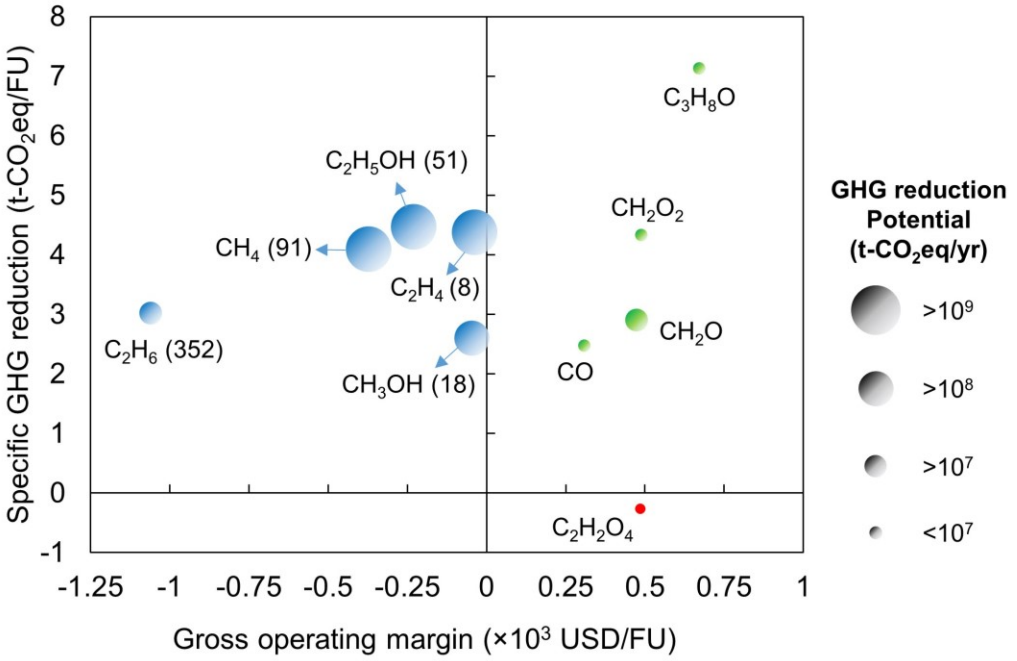

Figure 3. Evaluation results of ten electrochemical CO_2 conversion technologies on TRL 2 in the South Korean market. The functional unit is 1 ton of the target product and X ton of oxygen. The value of X depends on the target product. The size of the dots indicates the scale of their GHG reduction. Green: profitable and able to reduce GHG emissions. Red: profitable but unable to reduce GHG emissions. Blue: non-profitable but able to reduce GHG emissions. The numbers inside brackets are GHG avoidance costs (USD/t-CO_2eq). The evaluation results for another scenario that the oxygen byproduct cannot be sold but is vented into the environment are shown in Figure SI 1 of the ESI.

4. Case Study 2: Electrochemical Ethylene Production via Co-electrolysis of CO_2 and H_2O (TRL 2–4)

This case study shows how an electrochemical CO_2 conversion technology can be evaluated in the early-stage development and also demonstrates how the evaluation procedure and results evolve with increasing

TRL. More specifically, we discuss what primary data are additionally required, what secondary data should be calculated, and how close the value of the performance indicators at TRL 2 and 3 is to the value at TRL 4. To this end, we analyze the electrochemical production of ethylene via co-electrolysis of CO_2 and water. As analyzed in Case Study 1, ethylene is a promising CU product that has a high potential for GHG mitigation. Several lab-scale experiments have shown high performances, e.g., a high Faradaic efficiency toward ethylene [37–40], so we analyze this technology as if it were at TRL 2 to 4. Particularly at TRL 4, we conduct conceptual design of the separation process for CO_2 recovery and ethylene separation in order to calculate the secondary data.

4.1 Technology Description

As shown in Figure 4, the overall process for electrochemical ethylene production is composed of four parts. Similar to Case Study 1, CO_2 is captured at a coal-fired power plant via MEA-based absorption and supplied to the electrochemical membrane reactor (ECMR). At the anode half side of the reactor, process water is split to oxygen. At the cathode half side, CO_2 is reduced to ethylene, carbon monoxide, and methane and H^+ ions formed at the anode are reduced to hydrogen. The products from the cathode side are sent to separation stages where unreacted CO_2 is recovered for recycle and ethylene is purified. The residual chemical compounds in the off-gas are combusted. The ethylene production process is assumed to be implemented in South Korea as done in Case Study 1. More information on the technology can be found in Section 5.1 of the ESI.

Figure 4. A block flow diagram of the electrochemical ethylene production combined with the CO_2 capture process.

4.2 Primary Data Preparation

In the analysis at TRL 3 and 4, actual experimental data of ethylene production via electrochemical CO_2 reduction on a copper-based electrode are taken from Yano et al. [37] which represent a high Faradaic efficiency toward ethylene (~80%). Exclusively at TRL 4, additional primary data for the design of the separation process, such as the gas permeation unit of gas components and the price of membrane, are required. The list of the primary data required for this case study is given in Tables SI 7–9 of the ESI.

4.3 Secondary Data Calculation

We consider a production of 20 kton ethylene annually, i.e., a medium-scale chemical plant. We calculate mass balances of the co-electrolysis based on the stoichiometry of the electrochemical reactions. At TRL 3 and 4, we consider four major products, including ethylene, hydrogen, methane and carbon monoxide that amount to 97% of Faradaic efficiency. We calculate power demand for the co-electrolysis by using the measured cell potential and current density.

At TRL 3, we assume that the unreacted CO_2 and produced ethylene are fully recovered and thus no purge stream for CO_2 recycle is required. We calculate the minimal separation work for the CO_2 recovery and product separation. Only the total area of the electrolyzer cells is estimated. The off-gases are combusted but no heat recovery is applied.

At TRL 4, the separation process is rigorously designed using Aspen Custom Modeler® and Aspen Plus® as shown in Figure 5. To decrease the loss of ethylene in the membrane separation step, a two–stage membrane process is implemented, resulting in an ethylene recovery of 95%. Poly(ethylene glycol) diacrylate is chosen as membrane material for CO_2 removal [41]. The product-rich retentate stream of M11 is fed into an amine (MEA[42,43]) scrubbing process to remove residual CO_2. The purified stream is then separated in a cryogenic distillation process to maintain ethylene with a purity of 99.8%. Water is first separated from the gas stream in a flash in order to prevent ice formation in the distillation column (C2). This waste water is not recycled because of impurities that are not suitable for electrolysis. The purified ethylene is taken from the bottom part of the column, while the off-gases at the top of the column are combusted to produce low pressure steam. This steam is internally used for regeneration of the amine solvent. The size of the columns are estimated using Aspen Plus®.

The modeling and design of the ethylene production process for the TRL 3 and 4 analysis are elaborated in Section 5.3 of the ESI. Also, the calculated secondary data are given in Tables SI 11–14 of the ESI.

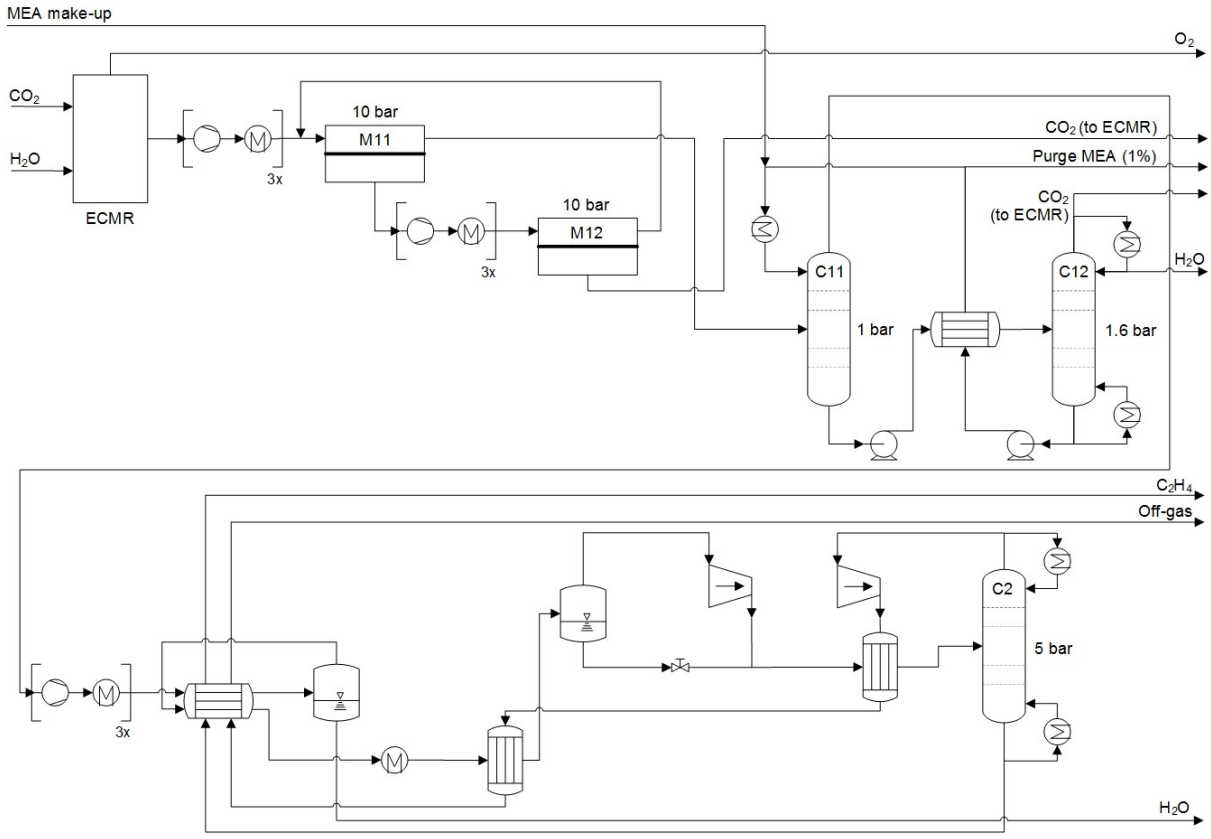

Figure 5: Process flowsheet for the electrochemical ethylene production developed for the analysis at TRL 4.

4.4 Evaluation Results

The functional unit is 1 ton of ethylene and X ton of oxygen. The value of X depends on the level of analysis as well as how the oxygen byproduct is treated. We analyze five performance indicators, including carbon utilization efficiency, exergy efficiency, gross operating margin (for TRL 2 only) or specific profit, specific GHG reduction, and GHG avoidance cost. Conventional production of ethylene via steam cracking of naphtha and of oxygen via cryogenic air separation are introduced as the reference. On the one hand, renewable electricity is generated by on-shore wind turbines and supplied to the electrolyzer cells continuously with the aid of batteries. On the other hand, for the CO_2 recovery and product purification, we define two scenarios: electricity is generated by on-shore wind turbines or taken from a power grid. This

scenario-based analysis shows how much the electricity source affects the accuracy of GHG reduction indicators. A cradle-to-gate system boundary is defined for LCA, which includes the GHG emissions from the raw material production (including CO_2 capture), purge stream, off-gas combustion, and renewable and grid electricity production. For the capital cost estimation at TRL 3 and 4, a global factor method [44] is applied. The process is assumed to be newly installed, so we use the formula for calculating the GHG avoidance cost applicable to the new installation case in Table 3. Equipment costs estimated at TRL 3 and 4 are given in Table SI 12 and Table SI 13 of the ESI, respectively.

Table 5 shows the performance indicators in the two scenarios. As the TRL increases, all the indicators become more accurate as the technology is analyzed more rigorously by accounting more for various nonideal factors. Therefore, GHG avoidance costs are increased while other indicators are decreased. Since renewable electricity is still expensive but ethylene is cheap, the specific profit is negative, which results in very high costs for GHG avoidance at TRL 3 and 4. Therefore, (1) utilization of cheap and clean electricity and (2) reduction in power consumption (i.e., toward lower overpotential) for the electrolysis should be aimed as they are hot spots. It is also noteworthy that the question of whether the oxygen byproduct is sold or vented into the air strongly affects the evaluation results, especially the GHG reduction indicators. The TEA and LCA for this scenario are described in Section 5.4 of the ESI.

Table 5. Performance indicators analyzed for the electrochemical ethylene production at TRL 2 to 4 for the two scenarios about the energy source for the product separation. The functional unit is 1 ton of ethylene and X ton of oxygen, where X varies depending on the level of the analysis.

Specification	**Source of electricity for separation process**					
	Wind (on-shore)			**Power grid**		
	TRL 2	**TRL 3**	**TRL 4**	**TRL 2**	**TRL 3**	**TRL 4**
Carbon utilization efficiency (%)	100	87.2	83.9	100	87.2	83.9
Exergy efficiency (%)	87.4[a]	35.2	31.2	87.4[a]	35.2	31.2
Specific GHG reduction (t-CO_2eq/FU)	4.37	4.13	4.02	4.37	4.06	2.10
Gross operating margin[b] / Specific profit[c] (M USD/FU)	-0.04	-4.43	-5.24	-0.04	-4.43	-5.17
GHG avoidance cost (USD/t-CO_2eq)	8.31	1,071	1,305	8.31	1,089	2,461

[a] Not 100% due to the energy demand for CO_2 capture.
[b] Calculated from the analysis at TRL 2.

[c] Calculated from the analyses at TRL 3 and 4.

The carbon utilization efficiency and exergy efficiency at TRL 3 are not significantly higher than those at TRL 4 because the loss of ethylene is very small and the separation energy demand is not as high as the electrolysis energy demand. Thus, accuracies of these two efficiencies at TRL 3 are comparable to those at TRL 4.

GHG reduction indicators are largely influenced by the carbon footprint of the energy required for non-reaction tasks if CO_2 conversion is driven by low carbon-intensive energy such as solar or wind power. When all the electronic equipment operates on renewable electricity, the specific GHG reduction at TRL 2 is higher than that at TRL 4 by only 8.7%. However, as shown in Figure 6, if grid electricity is supplied for the separation process, its indirect GHG emissions account for as much as 40.7% of the total emissions at TRL 4. As a result, the specific GHG reduction drops by more than a half and the GHG avoidance cost more than doubles as the TRL rises from 3 to 4. If the oxygen byproduct cannot be sold but is released into the environment, the specific GHG reduction becomes even negative (see Figure SI 5 of the ESI). The described effect is less pronounced when the energy driving CO_2 conversion reactions originates from carbon-intensive resources such as coal and natural gas. Therefore, the accuracy of the GHG reduction indicators at TRL 2 and 3 highly depends on what energy resources are utilized by the *entire* process.

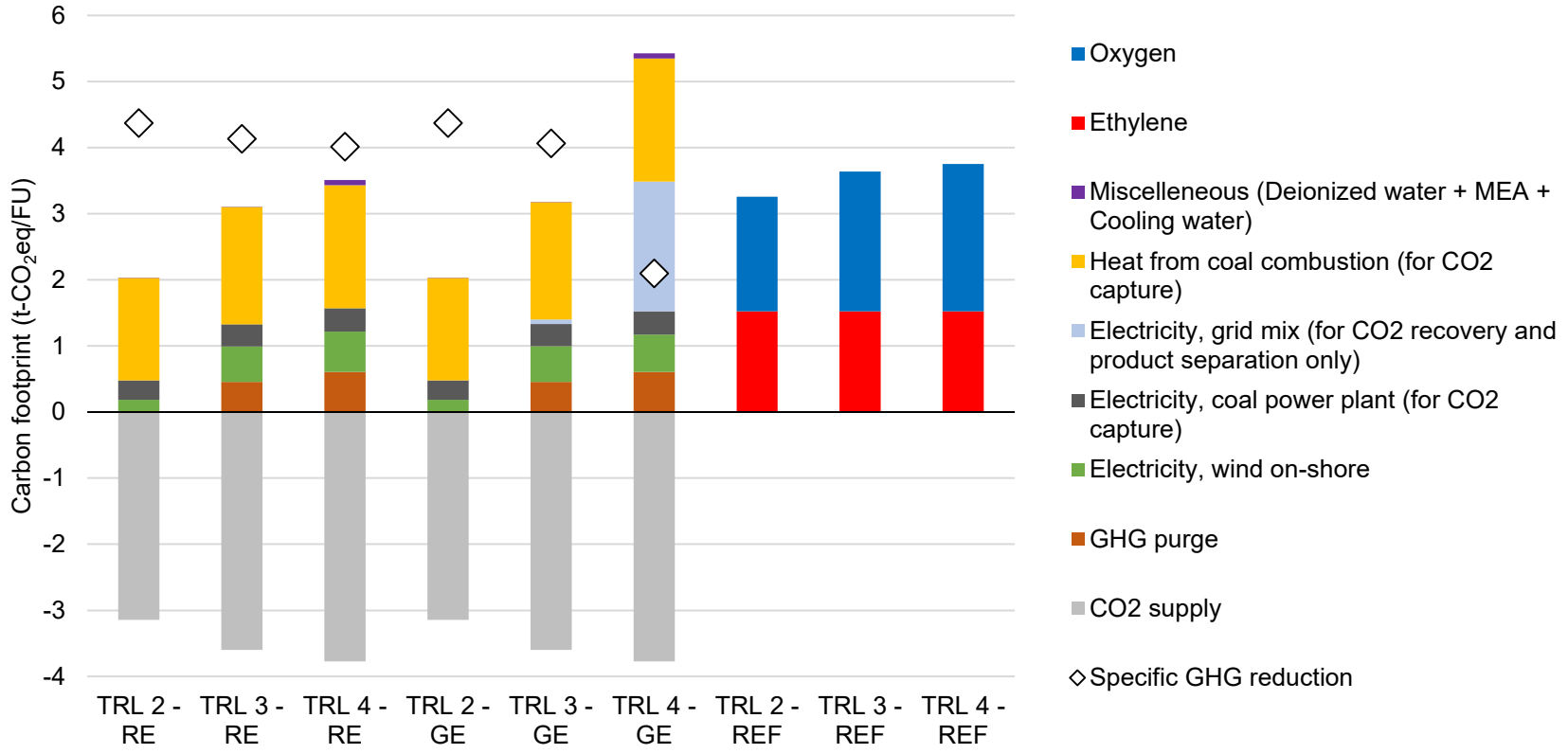

Figure 6. LCA results for the electrochemical ethylene production. The functional unit is 1 ton of ethylene and X ton of oxygen. The value of X depends on the level of the analysis. RE: Utilization of renewable electricity for the separation process. GE: Utilization of grid electricity for the separation process. REF: Reference production. CO_2 supply (gray) is plotted as a negative carbon footprint. The GHG reduction achieved by replacing the cryogenic air separation units is increased when TRL rises from 2 to 3 due to the side-products that increase the amount of oxygen byproduct.

The economic indicators analyzed at TRL 3 are relatively close to those at TRL 4 (e.g., 23.4% increase in the specific profit, S1). This can be attributed to the fact that the loss of ethylene is minimized and additional costs for the product separation are relatively smaller than the energy and depreciation costs for the electrolyzer cells. However, the cost indicator at TRL 2, namely direct operating cost, is far lower than the COGM at the higher TRLs. When the TRL increases from 2 to 3, the margin is significantly decreased due to the higher than twice requirement of the renewable electricity for electrolysis as well as the addition of the depreciation and indirect costs into the COGM (Figure 7). Therefore, the economic indicators at TRL 2 would only be useful when unpromising technologies should be quickly identified as in Case Study 1.

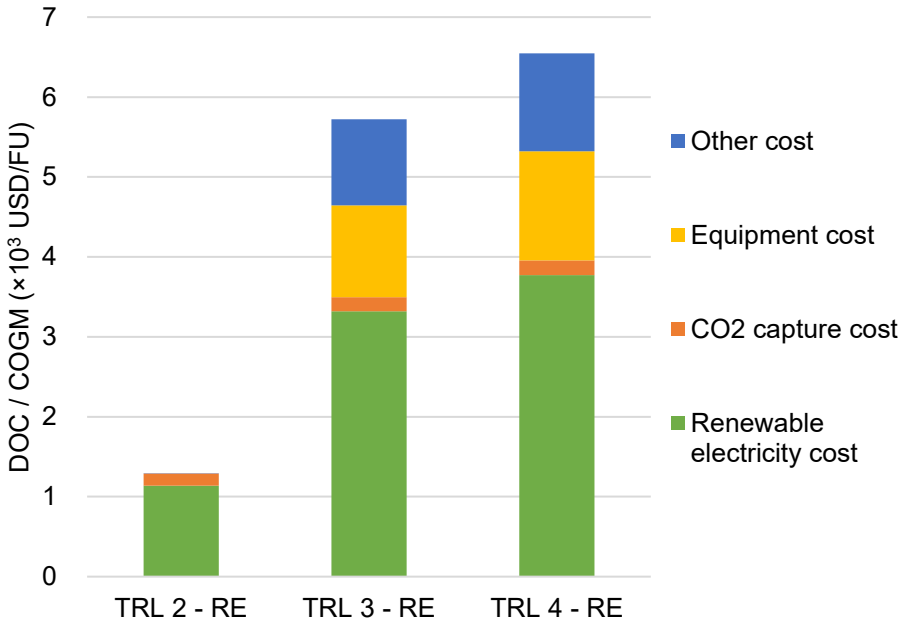

Figure 7. Direct operating cost (DOC) for the analysis at TRL 2 and cost of goods manufactured (COGM) for the analysis at TRL 3 and 4 of the electrochemical ethylene production in the case that renewable electricity is fully utilized in the whole process.

As given in Table 5, the GHG avoidance costs at low TRLs are highly uncertain. This is because this indicator is directly influenced by uncertainties in both the GHG reduction- and economics-related indicators. Therefore, it is recommended to analyze GHG avoidance costs at TRL 4 or higher.

Detailed description of the TEA and LCA results at TRL 4 is given in Section 5.4 of the ESI.

5. Case Study 3: Thermochemical CO_2 Conversion for OME_1 Production via Direct Oxidation of Methanol (TRL 4)

This case study evaluates a new process for the production of OME_1 ($CH_3OCH_2OCH_3$) as an example of thermochemical CO_2 conversion technologies by using the proposed procedure. OME_1 has recently attracted significant interest as a blend component for diesel fuel that can dramatically reduce the formation of soot and NO_x during combustion [45]. For the present work, selective direct oxidation of methanol ($3MeOH + 0.5O_2 \rightarrow OME_1 + 2H_2O$) [46] is considered as the target pathway for OME_1 formation, which involves fewer processing steps and requires less raw materials and energy than the established route via MeOH and formaldehyde [47]. Herein, the methanol feedstock originates from CO_2.

The concept of methanol oxidation to OME_1 is already validated in a laboratory environment since various studies have conducted catalyst development and improvement and have reported good reaction performance. Thus, the overall process is considered to be at TRL 4.

5.1 Technology Description

The process flow diagram of the OME_1 production process is depicted in Figure 8. Methanol is firstly synthesized from CO_2 and hydrogen via CO_2 hydrogenation ($CO_2 + 3H_2 \rightarrow MeOH + H_2O$) over a commercial $Cu/ZnO/Al_2O_3$ catalyst [48] in the reactor R1. Hydrogen is produced by a proton exchange membrane (PEM) electrolyzer. CO_2 could be obtained from various sources. As a best case scenario, we assume that CO_2 is available at no cost from an ethylene oxide plant, since these plants produce high purity CO_2 as an unused byproduct, which are currently released into the air [49]. Methanol is separated from water

in Distillation Column C1, and directly oxidized for the OME_1 synthesis over a $V_2O_5/TiO_2/SiO_2$ catalyst [50] in the reactor R2. Methyl formate (MF) and formaldehyde are the main side-products. All unreacted raw materials, by- and side-products are removed from OME_1 via distillation. Formaldehyde is converted to OME_1 at the reactive sections of C22 and C23. Although a market for the side-product MF exists, its disposal is not considered in this early evaluation. With a yield of less than 2%, MF formation is small; thus, its disposal has only a negligible influence on the overall result [50]. More information on the technology can be found in Section 6.1 of the ESI.

We consider Germany as an example of target markets in the European Union (EU). The EU has a large share of diesel engines even in passenger cars, and at the same time, there is increasing concern about the associated pollutant emissions, leading up to discussions about diesel driving bans. In 2019, about 3.8×10^7 tons of diesel fuel were sold in Germany [51]. Assuming a complete replacement with the OME_1-diesel blend as recommended by Omari et al. [45], which contains 24 wt.-% OME_1, this corresponds to a maximum market size in Germany of 9×10^6 t/yr. If deployed globally [52], the maximum market size would be 3×10^8 t/yr. The results of Deutz et al. [53] suggest that a similar fraction of the diesel-related GHG emissions can be saved if renewable raw materials are used.

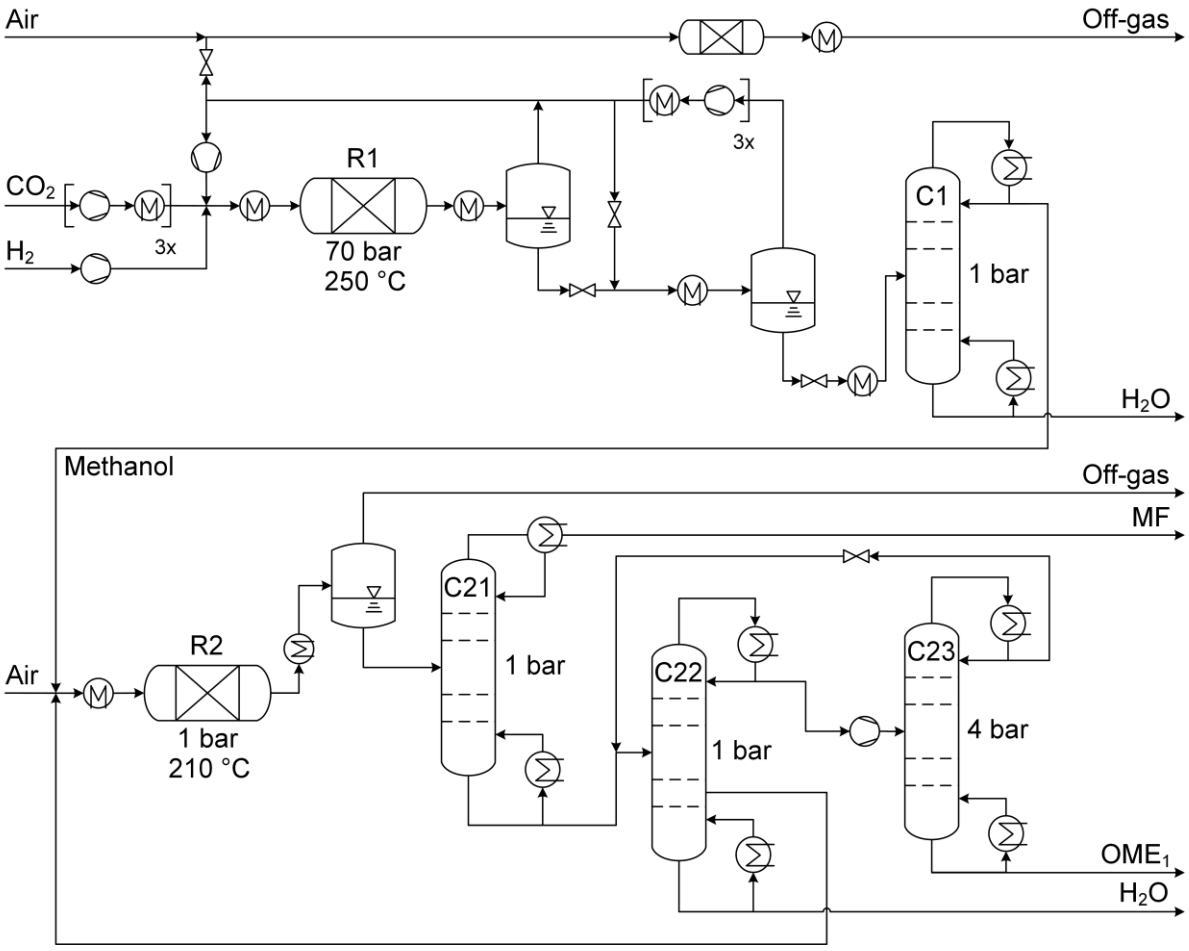

Figure 8. Process flow diagram for the oxidative OME_1 production from hydrogen and CO_2.

5.2 Primary Data Preparation

The TRL-dependent primary data are obtained from the open literature and database and relate to the two reactions such as operating conditions and reaction performances and the TRL-independent primary data, including the prices of raw materials, energy, and utilities (Table SI 16 of the ESI) and the life cycle inventory (LCI) datasets (Table SI 21 of the ESI). We introduce four scenarios: a baseline scenario with the reported reaction performances, two scenarios with the perturbed selectivity toward OME_1 (±5%) in R2,

and one ideal scenario indicating a theoretical limit calculated following the evaluation procedure for TRL 2 technology.

5.3 Secondary Data Calculation

We consider a production of 200 kton OME_1 annually, i.e., a large-scale chemical plant. Aspen Plus® is used for the process flowsheeting and mass and energy balance calculation. The first reaction is modeled using the reaction kinetics for a $Cu/ZnO/Al_2O_3$ catalyst [54] while the second reaction is modeled using a simple stoichiometry-based reactor model (RStoic in Aspen Plus®) with the experimental data (selective oxidation of methanol to OME_1 at low temperature over V_2O_5-TiO_2 catalysts) [50]. Unreacted raw materials are recycled, and pinch-based heat integration is applied, including off-gas combustion for energy recovery. Separation energy is calculated with the EE-ToolBox [55] using the Rectification Body Method [24], an intermediate-fidelity method which is based on the calculation of pinch points for the columns' rectification and stripping section. Based on mass and energy balances, an approximate sizing is conducted for major plant equipment such as distillation columns, reactors, compressors, and pumps. All the secondary data calculated can be found in Table SI 17–19 of the ESI.

5.4 Evaluation Results

Carbon utilization efficiency, exergy efficiency, COGM, and carbon footprint in the cradle-to-gate context are analyzed. The first two indicators are chosen for the comparison with the established OME_1 production with CO_2-based methanol production. The GHG emissions during equipment manufacturing, plant construction and deconstruction, and disposal of waste are excluded from the system boundary due to the lack of reliable data. As the price of OME_1 in the fuel market is unknown, we do not analyze the specific

profit and GHG avoidance costs. The functional unit is defined as 1 GJ (low heating value, LHV) of OME_1. Since some of the primary data are uncertain, we first calculate the performance indicators based on the nominal values and subsequently analyze sensitivity.

The carbon utilization efficiency and exergy efficiency are 93% and 76%, respectively, which are 3% (for both of the indicators) higher than the established OME_1 production [56]. This increase is due to the high selectivity of the present OME_1 production step from methanol as well as the tighter process integration. Including the energy demand for hydrogen production using the PEM electrolyzer, the overall exergy efficiency is 48% (compared to 47% in the established process).

The COGM is 66 EUR/GJ-OME_1, which is about twice the price of fossil diesel including tax (available in Germany in October 2018). With a hydrogen price of 4.5 EUR/kg-H_2, the hydrogen cost accounts for almost 95% of the COGM. As a result, the COGM strongly depends on the hydrogen price, as shown in Figure 9. In order to be economically viable, the hydrogen price needs to decrease below 3.6 EUR/kg-H_2 (based on the theoretical limit) and to 2.3 EUR/kg-H_2 (based on the TRL 4 results).

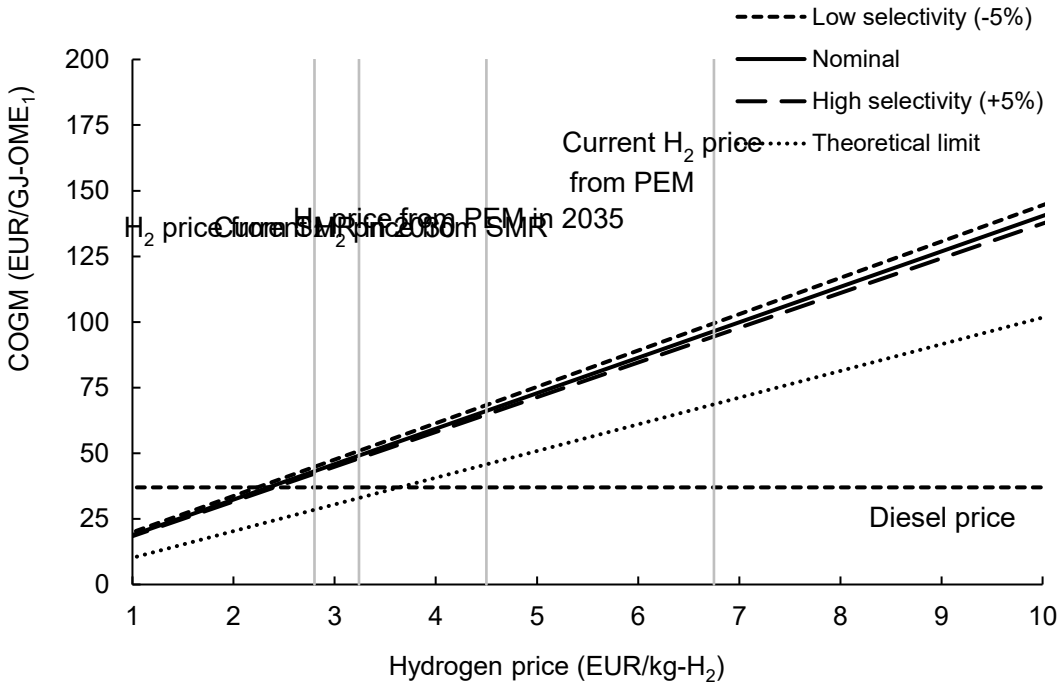

Figure 9. COGM of OME_1 on TRL 4 considering different values of the reaction selectivity toward OME_1 (nominal = 93%) and hydrogen prices.

The LCA results for the carbon footprint (Figure 10) depends strongly on the carbon footprint of electricity supply mainly for the hydrogen production. The results show that the oxidative OME_1 production could already reduce GHG emissions in several countries and the global forecasting grid mix in 2050 based on the 'beyond 2 °C scenario' by the IEA. Using the global forecasting grid mix for 2030, the carbon footprints of OME_1 are higher than diesel highlighting the importance of matching OME_1 production to renewable energy pathways.

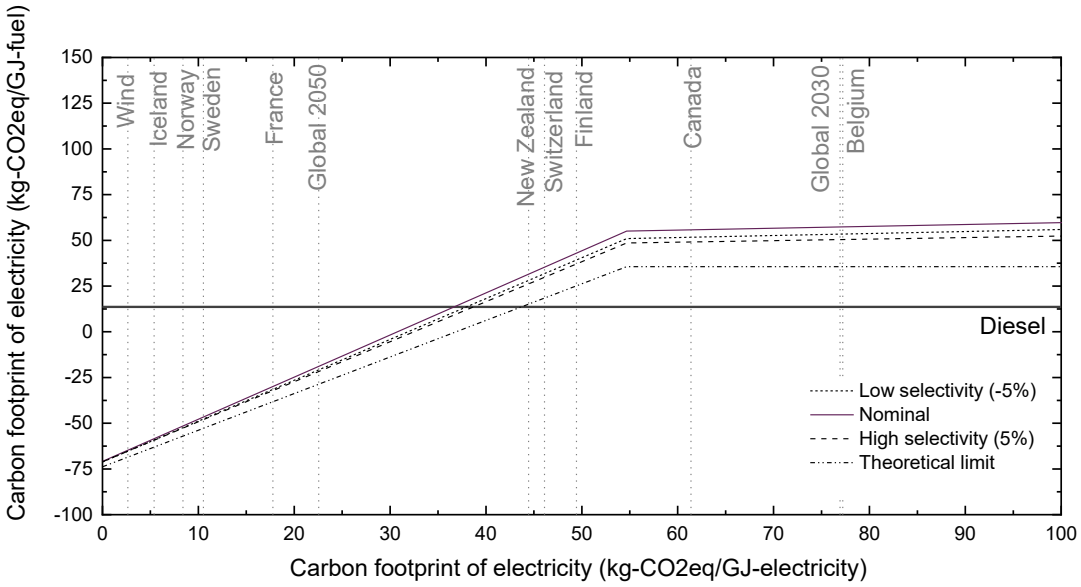

Figure 10. The carbon footprint from cradle-to-gate for the oxidative OME_1 production considering different values of the reaction selectivity toward OME_1 (nominal = 93%) and the fossil diesel over the GHG emissions of the electricity supply. The grey dashed lines represent the carbon footprint of various country-specific grid mixes and global forecasting grid mix for 2030 and 2050 based on the 'beyond 2°C scenario' of the IEA[57]. Up to 54.7 kg-CO_2eq/GJ-electricity (or 10.8 kg-CO_2eq/kg-H_2), hydrogen is provided by PEM-electrolysis then hydrogen production technology changes to steam methane reforming.

It is noted that recycling in the OME_1 production process minimizes the loss of the unreacted H_2. Therefore, the reaction selectivity towards OME_1, one of the key TRL-dependent primary data, influences the performance indicators less than other TRL-independent primary data, including the hydrogen price and the carbon footprint of electricity generation.

Discussion on the breakdowns of COGM and carbon footprints of the OME_1 production process can be found in Section 6.4 of the ESI.

6. Case Study 4: Biological CO_2 Conversion for Microalgal Biomass Co-Firing (TRL 4)

This case study considers the biological CO_2 conversion of direct combustion of solid microalgae, grown with CO_2 from flue gas. This technology can reduce the carbon footprint as well as maximize energy yield by effectively utilizing the entire biomass when the cultivation plant is integrated with an existing solid-firing power plant. This biological CO_2 conversion technology differs from the CU technologies in the other case studies. First, the technology is implemented to an existing power plant as a retrofit. Secondly, renewable electricity is not used as the main energy source, but solar energy and waste heat from low temperature flue gas. Lastly, experimental data coupled with empirical short-cut models are required for a process-level modeling of cultivation plants. Whereas classical microalgal growth models involve metabolic pathways with numerous reactions, it is difficult to justify their incorporation when process-scale growth models are able to sufficiently model biomass formation [58].

We rate microalgal biomass co-firing at TRL 4 based on the strategies employed for secondary data calculation, as outlined in Table 2, as well as the step-wise rating approach proposed by Buchner et al. [20]. With regards to the latter, the criteria of title and description befit that of TRL 4. The applications of shortcut bioprocess models for modeling algal growth kinetics have been met with some success, and current

development efforts focus on breadboard validations of the entire co-firing system at increasingly larger scales [59]. These bioprocess models mainly concern algal biomass growth rather than the co-firing technology as a whole, which includes downstream concentration, blowdown treatment, and pelletizing operations. A major challenge that remains to this date is the development of a multi-scale cultivation model that incorporates both microscopic cell properties with macroscopic reactor characteristics. Therefore, the current modeling approaches do not meet the completeness and robustness required for TRL 5. We evaluate this process by following the proposed procedure and compare its GHG avoidance cost to CCS.

6.1 Technology Description

Coal-fired power stations currently account for the single largest source of anthropomorphic GHG gas emissions, emitting over ten gigatons of CO_2 per year [60,61]. Despite this, coal-fired power plants continue to be built in developing countries, where the infrastructure and technology requirements for renewable energy sources are less likely to be met [62]. The main mitigation potential from algal biomass co-firing comes from the fact that upon full integration of the algal cultivation plant with an existing coal-fired power plant, the amount of CO_2 in circulation effectively becomes sequestered from the environment. As depicted in Figure 11, CO_2 in the post-combustion flue gas is fed directly to the cultivation plant as a raw material. For microalgal cultivation, modular and low-cost vertical airlift column photobioreactors with flue gas bubbling are considered. For the cultivating species, *Chlorella vulgaris* was selected due to its high productivity and moderately high low heating value [63]. Microalgal biomass is cultivated during the day and is harvested every two days in order to maximize temporal productivity. The harvested broth is pumped into a holding tank for concentration via electroflocculation. The broth is subsequently routed to a mixer-settler, after which solid-liquid separation removes the microalgal biomass from the bulk media. The resulting algal slurry undergoes belt filtration in which water is removed continuously and in multiple stages via a vacuum suction. Water is removed in a final drying step in a convective dryer, after which the biomass is pelletized.

Low temperature flue gas from the boiler stack (120–130 ºC) is routed to the belt dryer, and the waste heat is utilized to reduce the moisture content to below 10% [64].

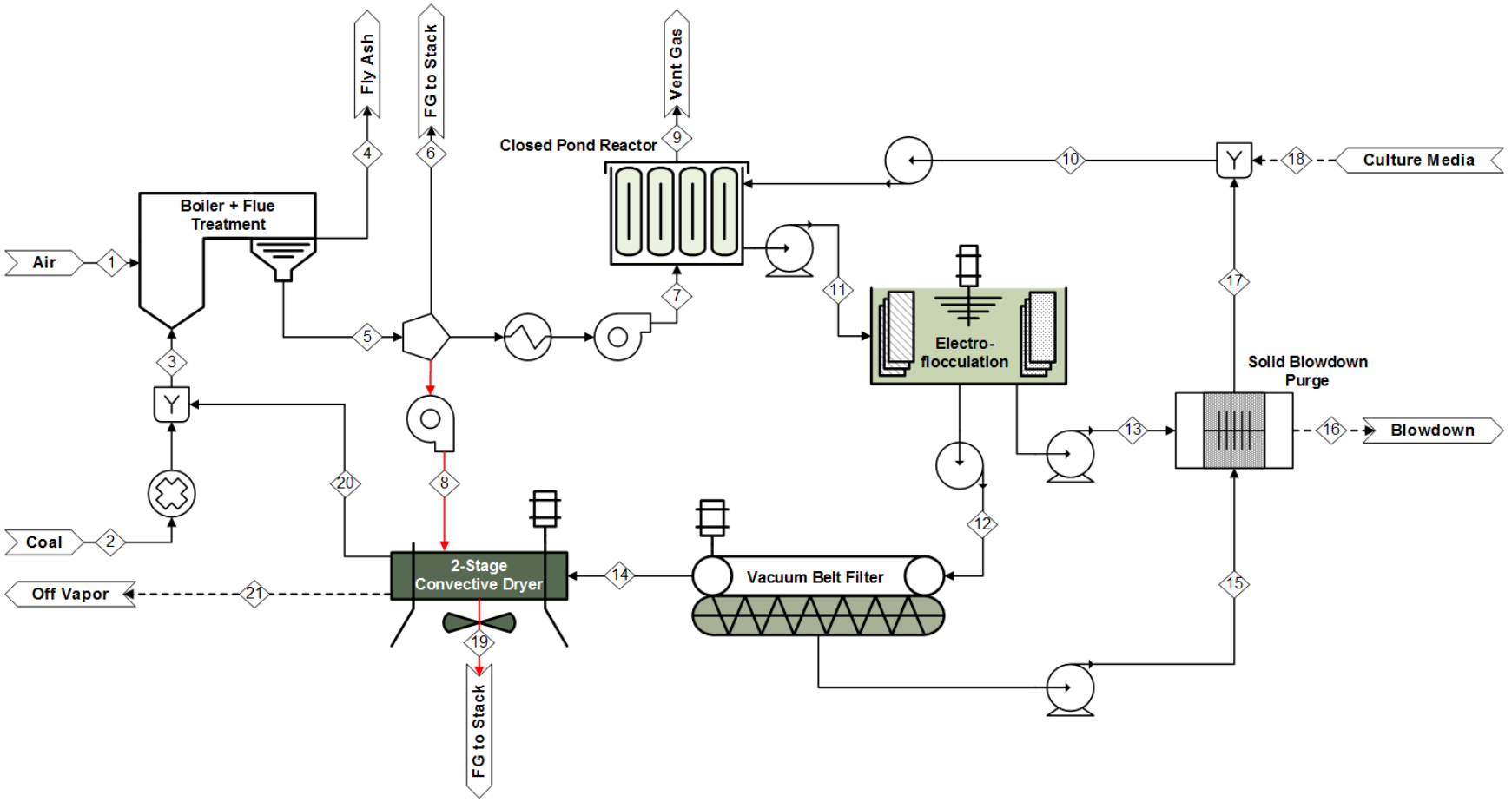

Figure 11. Process flow diagram of the microalgal cultivation plant for biomass co-firing with the major process equipment units. Dashed streams represent major water flows in/out of the process. Red streams represent flue gas stream for waste heat transfer.

6.2 Primary Data Preparation

Experimental data are taken from the open literature regarding the features of the microalgal biomass (e.g., low heating value of dried biomass), cultivation and harvest (e.g., biomass productivity, cultivation time, carbon utilization efficiency, and specific consumption of nutrients and energy), biomass separation (e.g., exit concentration, recovery rate, and specific consumption of energy); and equipment size parameters (Table SI 22 of the ESI).

6.3 Secondary Data Calculation

A 550 MW commercial coal power plant is assumed in the Southwestern United States utilizing ultra-supercritical coal. This geographical area is suitable for a large-scale microalgae cultivation because of the presence of a reservoir, plenty of unused lands, and high solar irradiation [65]. The base co-firing fraction is 10%, meaning that microalgal biomass to the boiler in the power plant has to supply 10% of the total boiler energy input. To calculate mass balances, a component balance model [66] is constructed in which the basic mass units are compounds rather than chemical elements. Energy and utility consumptions for the cultivation and electro-flocculation processes are calculated by linearly scaling large-scale pilot plant data available. Conventional process equipment such as pumps and heat exchangers are analyzed by using widely available models or empirical relationships. The calculated secondary data can be found in Table SI 24 and 26 of the ESI.

6.4 Evaluation Results

The carbon utilization efficiency, levelized cost of electricity, as an alternative to COGM, carbon footprint, and GHG avoidance cost are analyzed. Energy indicators are not analyzed because the main energy resource (i.e., solar energy) is free. The GHG emissions during equipment manufacturing, plant

construction and deconstruction, and disposal of waste are excluded from the system boundary due to the lack of reliable data. Since an existing power plant is retrofitted, we use the formula for the GHG avoidance cost calculation applicable to the retrofitting case in Table 3. The functional unit is defined as 1 GJ of electricity generated. Details of the TEA and LCA conducted are described in Section 7.4 of the ESI. Since some of the primary data are uncertain, we first calculate the performance indicators based on the nominal values and subsequently analyze sensitivity.

The carbon utilization efficiency is only 36%. Only a part of the carbon in the flue gas is dissolved in media and converted into microalgal biomass. Also, around 23% of the carbon in the cultivated biomass is lost during the biomass recovery. Details of the carbon flow are described in Figure SI 10 of the ESI. The LCOE is 33.6 USD/GJ (see the breakdown in Figure SI 9 of the ESI) compared to 31.4 USD/GJ for the coal-fired power plant with no co-firing. Despite the 7% increase due to the microalgal plant installed, the LCOE is still well within the current range for coal-fired power plants in the United States (from 20.6 USD/GJ to 37.5 USD/GJ) [67]. The co-firing plant reduces the carbon footprint to 0.19 t-CO_2eq/GJ from 0.26 ton-CO_2eq/GJ (no co-firing). The baseline GHG avoidance cost, which is calculated when all primary and secondary data are incorporated at their face value without consideration of uncertainty, is 26.7 USD/t-CO_2eq. This value is comparable with the currently reported GHG avoidance costs for CCS (see Section 3.4). Therefore, microalgal co-firing can be considered as an economically viable option for CU.

A sensitivity analysis was performed by perturbing the model parameters and observing their effect on the baseline GHG avoidance cost at 26.7 USD/t-CO_2eq. Figure 12 shows that with respect to several endogenous uncertainties, the recovery of biomass at downstream, raw material cost, and low heating value of microalgal biomass most significantly influence the GHG avoidance cost. In particular, the significance of the biomass recovery agrees with the results of the carbon utilization efficiency analysis. Therefore, such hotspots should be the main research targets at higher TRLs. Also, differently from the previous case studies, the performance indicators at TRL 3 will become very inaccurate if perfect separation is assumed. Therefore, it is critical to assume a reasonable value of product recovery for this kind of CU technologies. Since this

system mainly relies on the utilization of the waste heat from the flue gas, the effect of exogenous uncertainty is limited, in contrast to the CU technologies in the other case studies. The sensitivity analysis is elaborated in Section 7.5 in the ESI.

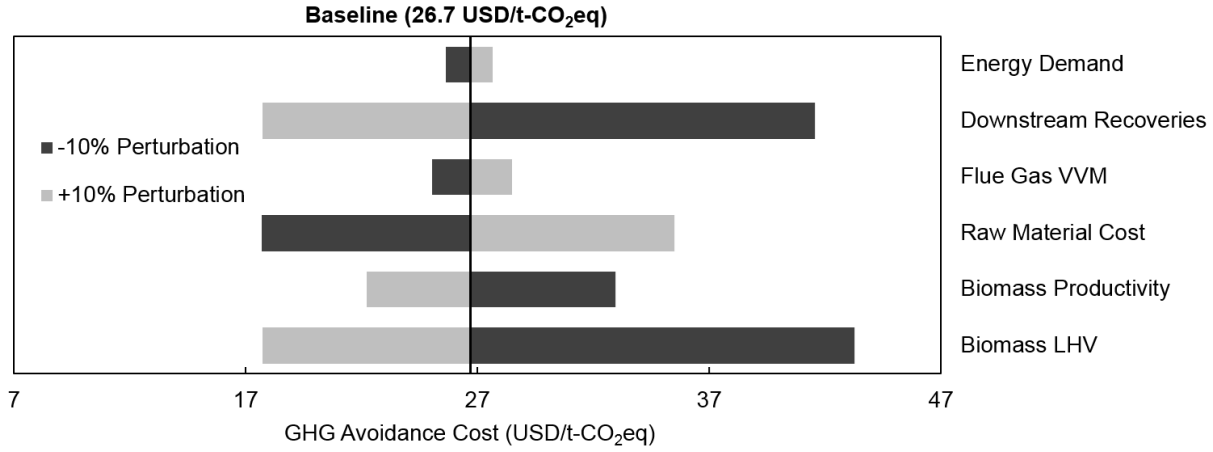

Figure 12. Sensitivity analysis results of major plant parameters (±10% changes) with respect to the GHG avoidance cost. The break at 26.7 USD/t-CO_2eq represents the baseline GHG avoidance cost.

7. Conclusion and Outlook

We proposed a systematic procedure for early-stage evaluations of CU technologies at low TRLs. The procedure obtains performance indicators in three steps: primary data preparation, secondary data calculation, and performance indicator calculation. The first two steps differ according to the TRL as well as the type of CO_2 conversion. Furthermore, we presented a number of databases, methods, and computer-aided tools that can effectively support the procedure.

We conducted four case studies to illustrate the procedure as well as to assess the specific emerging CU technologies and obtain three key findings. i) Two unpromising routes (producing ethane and oxalic acid) out of ten electrochemical CO_2 reduction technologies were excluded using stoichiometry-based methods.

ii) The price and carbon footprint of renewable energy/raw materials play central roles in the electrochemical ethylene production and thermochemical OME_1 production. In the current market situation, the economic viability of these two CU technologies is not guaranteed. iii) Microalgae biomass co-firing is sustainable as it mainly utilizes free and clean energy for biological CO_2 conversion. The biomass recovery is found to be a key parameter that largely affects the performance indicators.

We also point out that the accuracy of the performance indicators at TRL 2 and 3 strongly depends on (1) what type of energy is supplied to the *entire* CCU system and (2) how much of the CU product can be recovered in reality. Furthermore, GHG avoidance costs can be highly underestimated at TRL 2 and 3 and are therefore only recommended as performance indicators at TRL 4 or higher.

In addition to the three types of CO_2 conversion that we investigated, there exist many other types of CU technologies, such as plasma-based conversion, photo-electrochemical conversion, and mineralization. These remaining technologies can likely be assessed following the proposed procedure but demand different methods for calculating the secondary data. Also, an evaluation procedure tailored to emerging CO_2 capture technologies needs to be established. Furthermore, on top of carbon footprint, other environmental impacts such as fossil-fuel depletion and water footprint need to be addressed.

The intent of the proposed procedure is to suggest a foundation and a unified framework for early-stage evaluations of a variety of emerging CU technologies. However, some subjective judgments are inevitable during the evaluation, e.g., to characterize the uncertainty of the primary data based on theoretical evidence or expert's intuition. One particular example is the comparison of CU technologies at different TRLs. This task is not straightforward because each TRL demands different procedures for calculating the performance indicators, as shown in Table 2. Also, the expected range of the performance indicators for low TRL technologies is broader than that for high TRL technologies. Low TRL technologies might (or have to) be significantly improved through future R&D until they are commercialized. Still, it is difficult to do so for

high TRL technologies as they are already at an optimized state. As future work, we plan to develop a systematic approach for such a comparison to help avoid misguided decision-making.

Acknowledgement

The authors gratefully acknowledge funding by the German Federal Ministry of Education and Research (BMBF) within the Kopernikus-project SynErgie and the project supervision by the project management organization Projektträger Jülich (PtJ). This work was funded by BMBF within the Kopernikus Project P2X: Flexible use of renewable resources – exploration, validation and implementation of 'Power-to-X' concepts. This work was funded by the Deutsche Forschungsgemeinschaft (DFG, German Research Foundation) under Germany's Excellence Strategy – Cluster of Excellence 2186 "The Fuel Science Center" – ID: 390919832. The authors also acknowledge the financial support from Korea Carbon Capture & Sequestration R&D Center (KCRC) under the project #NRF 2015M1A8A1076118. The authors are also grateful to Jaeseo Lee for fruitful discussions on the analysis of the electrochemical CO_2 reduction technologies.

Author Contributions

K.R. proposed the evaluation procedures and D.B., J.B., A.K., A.B. and A.M. thoroughly reviewed them. K.R., D.B., J.B. and A.K. compiled and described the databases, methods, and computer-aided tools. K.R., D.B., J.B., S.D., W.C., D.H., M.H., S.V., R.M., and J.S.L. selected and defined case studies. K.R., W.C., D.H. and J.H.L. screened the ten electrochemical CO_2 reduction technologies. K.R., W.C., D.H. and J.H.L. evaluated the ethylene production process at TRL 3. A.B., M.H., Y.K., R.M., S.V. and M.W. designed and evaluated the ethylene production process at TRL 4. J.B., D.B., S.D., A.B. and A.M designed and evaluated the OME_1 production process. J.S.L. and J.H.L. designed and evaluated the microalgal co-firing process. All authors contributed to writing and editing the manuscript.

References

1 A. W. Zimmermann and R. Schomäcker, Assessing Early-Stage CO_2 utilization Technologies—Comparing Apples and Oranges?, *Energy Technol.*, 2017, **5**, 850–860.

2 K. Roh, A. S. Al-Hunaidy, H. Imran and J. H. Lee, Optimization-based identification of CO_2 capture and utilization processing paths for life cycle greenhouse gas reduction and economic benefits, *AIChE J.*, 2019, **65**, e16580.

3 Wilf Lytton, CCU-fuels are not renewable, https://sandbag.org.uk/2016/11/27/ccu-fuels-are-not-renewable/, (accessed 17 May 2019).

4 A. Kätelhön, R. Meys, S. Deutz, S. Suh and A. Bardow, Climate change mitigation potential of carbon capture and utilization in the chemical industry, *Proc. Natl. Acad. Sci.*, 2019, **116**, 11187–11194.

5 J. Artz, T. E. Müller, K. Thenert, J. Kleinekorte, R. Meys, A. Sternberg, A. Bardow and W. Leitner, Sustainable Conversion of Carbon Dioxide: An Integrated Review of Catalysis and Life Cycle Assessment, *Chem. Rev.*, 2018, **118**, 434–504.

6 A. Otto, T. Grube, S. Schiebahn and D. Stolten, Closing the loop: captured CO_2 as a feedstock in the chemical industry, *Energy Environ. Sci.*, 2015, **8**, 3283–3297.

7 K. Roh, R. Frauzem, R. Gani and J. H. Lee, Process systems engineering issues and applications towards reducing carbon dioxide emissions through conversion technologies, *Chem. Eng. Res. Des.*, 2016, **116**, 27–47.

8 Carbon Recycling International, Carbon Recycling International, http://www.carbonrecycling.is/, (accessed 6 June 2018).

9 S. Rönsch, J. Schneider, S. Matthischke, M. Schlüter, M. Götz, J. Lefebvre, P. Prabhakaran and S. Bajohr, Review on methanation – From fundamentals to current projects, *Fuel*, 2016, **166**, 276–296.

10 Sunfire GmbH, Sunfire - Syngas, https://www.sunfire.de/en/, (accessed 9 June 2018).

11 M. Aresta, A. Dibenedetto and E. Quaranta, State of the art and perspectives in catalytic processes for CO_2 conversion into chemicals and fuels: The distinctive contribution of chemical catalysis and biotechnology, *J. Catal.*, 2016, **343**, 2–45.

12 A. Zimmermann, J. Wunderlich, G. Buchner, L. Müller, K. Armstrong, S. Michailos, A. Marxen, H. Naims, F. Mason, G. Stokes and E. Williams, *Techno-Economic Assessment & Life-Cycle Assessment Guidelines for CO_2 Utilization*, 2018.

13 J. Black, *Cost and performance metrics used to assess carbon utilization and storage technologies*, 2014.

14 W. Schakel, C. Fernández-Dacosta, M. van der Spek and A. Ramírez, New indicator for comparing the energy performance of CO_2 utilization concepts, *J. CO2 Util.*, 2017, **22**, 278–288.

15 K. Roh, H. Lim, W. Chung, J. Oh, H. Yoo, A. S. Al-Hunaidy, H. Imran and J. H. Lee, Sustainability analysis of CO_2 capture and utilization processes using a computer-aided tool, *J. CO2 Util.*, 2018, **26**, 60–69.

16 F. G. Albrecht, D. H. König, N. Baucks and R.-U. Dietrich, A standardized methodology for the

techno-economic evaluation of alternative fuels – A case study, *Fuel*, 2017, **194**, 511–526.

17 J. A. Bergerson, A. Brandt, J. Cresko, M. Carbajales-Dale, H. L. MacLean, H. S. Matthews, S. McCoy, M. McManus, S. A. Miller, W. R. Morrow, I. D. Posen, T. Seager, T. Skone and S. Sleep, Life cycle assessment of emerging technologies: Evaluation techniques at different stages of market and technical maturity, *J. Ind. Ecol.*, 2019, jiec.12954.

18 G. Thomassen, M. Van Dael, S. Van Passel and F. You, How to assess the potential of emerging green technologies? Towards a prospective environmental and techno-economic assessment framework, *Green Chem.*, 2019, **21**, 4868–4886.

19 M. Héder, From NASA to EU: the evolution of the TRL scale in Public Sector Innovation, *Innov. J.*, 2017, **22**, 1–23.

20 G. A. Buchner, K. J. Stepputat, A. W. Zimmermann and R. Schomäcker, Specifying Technology Readiness Levels (TRL) for the Chemical Industry, *Ind. Eng. Chem. Res.*, 2019, acs.iecr.8b05693.

21 ICIS, ICIS Petrochemical Index (IPEX), https://www.icis.com/about/ipex/#, (accessed 9 October 2018).

22 Chemical Engineering, The Chemical Engineering Plant Cost Index, https://www.chemengonline.com/pci-home, (accessed 9 October 2018).

23 J. M. Douglas, A hierarchical decision procedure for process synthesis, *AIChE J.*, 1985, **31**, 353–362.

24 J. Bausa, R. v. Watzdorf and W. Marquardt, Shortcut methods for nonideal multicomponent distillation: I. Simple columns, *AIChE J.*, 1998, **44**, 2181–2198.

25 H. Yeomans and I. E. Grossmann, A systematic modeling framework of superstructure optimization in process synthesis, *Comput. Chem. Eng.*, 1999, **23**, 709–731.

26 B. Bao, D. K. S. Ng, D. H. S. Tay, A. Jiménez-Gutiérrez and M. M. El-Halwagi, A shortcut method for the preliminary synthesis of process-technology pathways: An optimization approach and application for the conceptual design of integrated biorefineries, *Comput. Chem. Eng.*, 2011, **35**, 1374–1383.

27 A. Voll and W. Marquardt, Reaction network flux analysis: Optimization-based evaluation of reaction pathways for biorenewables processing, *AIChE J.*, 2012, **58**, 1788–1801.

28 K. Ulonska, M. Skiborowski, A. Mitsos and J. Viell, Early-stage evaluation of biorefinery processing pathways using process network flux analysis, *AIChE J.*, 2016, **62**, 3096–3108.

29 D. Schack, L. Rihko-Struckmann and K. Sundmacher, Linear Programming Approach for Structure Optimization of Renewable-to-Chemicals (R2Chem) Production Networks, *Ind. Eng. Chem. Res.*, 2018, **57**, 9889–9902.

30 M.-O. Bertran, R. Frauzem, A.-S. Sanchez-Arcilla, L. Zhang, J. M. Woodley and R. Gani, A generic methodology for processing route synthesis and design based on superstructure optimization, *Comput. Chem. Eng.*, 2017, **106**, 892–910.

31 A. König, K. Ulonska, A. Mitsos and J. Viell, Optimal Applications and Combinations of Renewable Fuel Production from Biomass and Electricity, *Energy & Fuels*, 2019, **33**, 1659–1672.

32 A. Sternberg and A. Bardow, Power-to-What? – Environmental assessment of energy storage systems, *Energy Environ. Sci.*, 2015, **8**, 389–400.

33 O. G. Sánchez, Y. Y. Birdja, M. Bulut, J. Vaes, T. Breugelmans and D. Pant, Recent advances in industrial CO_2 electroreduction, *Curr. Opin. Green Sustain. Chem.*, 2019, **16**, 47–56.

34 Knoema, Republic of Korea - CO_2 emissions, https://knoema.com/atlas/Republic-of-Korea/CO2-emissions, (accessed 6 March 2020).

35 Minister of Trade Industry and Energy, The 8th Basic Plan for Long-term Electricity Supply and Demand in Korea, 2017.

36 E. S. Rubin, J. E. Davison and H. J. Herzog, The cost of CO_2 capture and storage, *Int. J. Greenh. Gas Control*, 2015, **40**, 378–400.

37 H. Yano, T. Tanaka, M. Nakayama and K. Ogura, Selective electrochemical reduction of CO_2 to ethylene at a three-phase interface on copper(I) halide-confined Cu-mesh electrodes in acidic solutions of potassium halides, *J. Electroanal. Chem.*, 2004, **565**, 287–293.

38 J.-B. Vennekoetter, R. Sengpiel and M. Wessling, Beyond the catalyst: How electrode and reactor design determine the product spectrum during electrochemical CO_2 reduction, *Chem. Eng. J.*, 2019, **364**, 89–101.

39 J.-B. Vennekötter, T. Scheuermann, R. Sengpiel and M. Wessling, The electrolyte matters: Stable systems for high rate electrochemical CO_2 reduction, *J. CO2 Util.*, 2019, **32**, 202–213.

40 C.-T. Dinh, T. Burdyny, M. G. Kibria, A. Seifitokaldani, C. M. Gabardo, F. P. García de Arquer, A. Kiani, J. P. Edwards, P. De Luna, O. S. Bushuyev, C. Zou, R. Quintero-Bermudez, Y. Pang, D. Sinton and E. H. Sargent, CO_2 electroreduction to ethylene via hydroxide-mediated copper catalysis at an abrupt interface, *Science (80-.).*, 2018, **360**, 783–787.

41 H. Lin and B. D. Freeman, Gas Permeation and Diffusion in Cross-Linked Poly(ethylene glycol diacrylate), *Macromolecules*, 2006, **39**, 3568–3580.

42 Y. Zhang, H. Que and C.-C. C. Chen, Thermodynamic modeling for CO_2 absorption in aqueous MEA solution with electrolyte NRTL model, *Fluid Phase Equilib.*, 2011, **311**, 67–75.

43 H. Hikita, S. Asai, H. Ishikawa and M. Honda, The kinetics of reactions of carbon dioxide with monoethanolamine, diethanolamine and triethanolamine by a rapid mixing method, *Chem. Eng. J.*, 1977, **13**, 7–12.

44 G. A. Buchner, A. W. Zimmermann, A. E. Hohgräve and R. Schomäcker, Techno-economic Assessment Framework for the Chemical Industry—Based on Technology Readiness Levels, *Ind. Eng. Chem. Res.*, 2018, **57**, 8502–8517.

45 A. Omari, B. Heuser and S. Pischinger, Potential of oxymethylenether-diesel blends for ultra-low emission engines, *Fuel*, 2017, **209**, 232–237.

46 G. Busca, A. S. Elmi and P. Forzatti, Mechanism of selective methanol oxidation over vanadium oxide-titanium oxide catalysts: a FT-IR and flow reactor study, *J. Phys. Chem.*, 1987, **91**, 5263–5269.

47 J.-O. Weidert, J. Burger, M. Renner, S. Blagov and H. Hasse, Development of an Integrated Reaction–Distillation Process for the Production of Methylal, *Ind. Eng. Chem. Res.*, 2017, **56**, 575–582.

48 K. M. V. Bussche and G. F. Froment, A Steady-State Kinetic Model for Methanol Synthesis and the Water Gas Shift Reaction on a Commercial $Cu/ZnO/Al_2O_3$ Catalyst, *J. Catal.*, 1996, **161**, 1–10.

49 J. C. M. Farla, C. A. Hendriks and K. Blok, Carbon dioxide recovery from industrial processes, *Energy Convers. Manag.*, 1995, **36**, 827–830.

50 Q. Sun, J. Liu, J. Cai, Y. Fu and J. Shen, Effect of silica on the selective oxidation of methanol to dimethoxymethane over vanadia–titania catalysts, *Catal. Commun.*, 2009, **11**, 47–50.

51 Mineralölwirtschaftsverband, MINERAL-ÖL-AB-SATZ, https://www.mwv.de/statistiken/mineraloelabsatz/, (accessed 25 February 2020).

52 OECD/IEA, Oil final consumption by product, World 1990-2017, https://www.iea.org/data-and-statistics?country=WORLD&fuel=Oil&indicator=Crude oil imports vs. exports, (accessed 25 February 2020).

53 S. Deutz, D. Bongartz, B. Heuser, A. Kätelhön, L. Schulze Langenhorst, A. Omari, M. Walters, J. Klankermayer, W. Leitner, A. Mitsos, S. Pischinger and A. Bardow, Cleaner production of cleaner fuels: wind-to-wheel – environmental assessment of CO_2-based oxymethylene ether as a drop-in fuel, *Energy Environ. Sci.*, 2018, **11**, 331–343.

54 É. S. Van-Dal and C. Bouallou, Design and simulation of a methanol production plant from CO_2 hydrogenation, *J. Clean. Prod.*, 2013, **57**, 38–45.

55 AVT, EE-Toolbox, http://www.avt.rwth-aachen.de/cms/AVT/Forschung/Software/~iptv/Shortcut-Toolbox/?lidx=1, (accessed 16 October 2018).

56 D. Bongartz, J. Burre and A. Mitsos, Production of Oxymethylene Dimethyl Ethers from Hydrogen and Carbon Dioxide—Part I: Modeling and Analysis for OME 1, *Ind. Eng. Chem. Res.*, 2019, **58**, 4881–4889.

57 IEA and International Energy Agency, *Energy Technology Perspectives 2017*, OECD, 2017.

58 K. H. Ryu, B. Kim and J. H. Lee, A model-based optimization of microalgal cultivation strategies for lipid production under photoautotrophic condition, *Comput. Chem. Eng.*, 2019, **121**, 57–66.

59 S. Tebbani, F. Lopes, R. Filali, D. Dumur and D. Pareau, *CO_2 Biofixation by Microalgae*, John Wiley & Sons, Inc., Hoboken, NJ, USA, 2014.

60 OECD/IEA, *Global Energy & CO_2 Status Report 2018*, Paris, France, 2019.

61 BP, *BP Statistical Review of World Energy*, London, UK, 2019.

62 M. Brown and T. Buckley, IEEFA China: Lender of last resort for coal plants, *IEEFA*, 2019.

63 S. Al-lwayzy, T. Yusaf and R. Al-Juboori, Biofuels from the Fresh Water Microalgae Chlorella vulgaris (FWM-CV) for Diesel Engines, *Energies*, 2014, **7**, 1829–1851.

64 H. Li, Q. Chen, X. Zhang, K. N. Finney, V. N. Sharifi and J. Swithenbank, Evaluation of a biomass drying process using waste heat from process industries: A case study, *Appl. Therm. Eng.*, 2012, **35**, 71–80.

65 K. L. Kadam, *Microalgae Production from Power Plant Flue Gas: Environmental Implications on a Life Cycle Basis*, Golden, Colorado, 2001.

66 E. H. Dunlop and A. K. Coaldrake, Techno-economic modelling of algal processes with Aspen, in *ABO Algal Biomass Summit*, San Diego, CA, 2014.

67 NREL OpenEI, Transparent Cost Database, https://openei.org/apps/TCDB/transparent_cost_database, (accessed 1 November 2018).